Heavy Deformation and High-Temperature Annealing Microstructure and Texture Studies of TaHfNbZrTi Equiatomic Refractory High Entropy Alloy

Veeresham Mokali

***Abstract*—**The refractory alloys are crucial for high-temperature applications to improve performance and reduce cost. They are used in several applications such as aerospace, outer space, military and defense, nuclear powerplants, automobiles, and industry. The conventional refractory alloys show greater stability at high temperatures and in contrast they have operational limitations due to their low melting temperatures. However, there is a huge requirement to improve the refractory alloys' operational temperatures and replace the conventional alloys. The newly emerging refractory high entropy alloys (RHEAs) could be alternative materials for conventional refractory alloys and fulfill the demands and requirements of various practical applications in the future. The RHEA TaHfNbZrTi was prepared through an arc melting process. The annealing behavior of severely deformed equiatomic RHEATaHfNbZrTi has been investigated. To obtain deformed condition, the alloy is cold-rolled to 90% thickness reduction and then subjected to an annealing process to observe recrystallization and microstructural evolution in the range of 800 °C to 1400 °C temperatures. The cold-rolled – 90% condition shows the presence of microstructural heterogeneity. The annealing microstructure of 800 °C temperature reveals that partial recrystallization and further annealing treatment carried out annealing treatment in the range of 850 °C to 1400 °C temperatures exhibits completely recrystallized microstructures, followed by coarsening with a degree of annealing temperature. The deformed and annealed conditions featured the development of body-centered cubic (BCC) fiber textures. The experimental investigation of heavy deformation and followed by high-temperature annealing up to 1400 °C temperature will contribute to the understanding of microstructure and texture evolution of emerging RHEAs.

***Keywords*—**Refractory high entropy alloys, cold-rolling, annealing, microstructure, texture.

I. Introduction

THE 'high entropy alloys' (HEAs), a new class of alloys, emerged in the last decade. The increase in the number (more than four) of alloying elements leads to the enhancement of the system's configurational entropy. The HEAs are consisting of higher configurational entropy, which helps in stabilizing simple solid solutions like body-centered cubic (BCC), face-centered cubic (FCC), and BCC+FCC and also hinders harmful intermetallic phases [1]-[4]. Over the period, researchers gave different names to these alloys know as multi-component alloys, complex concentrated alloys, etc. Due to its attractive various mechanical properties and other functional properties, the domain of HEA materials has been expanded to high entropy ceramics, high entropy biomaterials, high entropy oxides and nitrides, high entropy-based coating, etc. HEAs show unique properties over conventional alloys, and the uniqueness is because of high configurational entropy, severe lattice distortion, cocktail effect, and sluggish diffusion. The high entropy materials have attracted research interest enormously due to their many impressive properties [5]-[12]. Sluggish diffusion property in HEAs reduces the kinetics of diffusion and increases the activation energy. The sluggish diffusion in HEA helps develop refractory materials for various high-temperature applications. After that, further high-temperature properties along with the melting point of these RHEAs alloys anticipated to improve by choosing the high melting point individual refractory elements, i.e., group IV (Hf, Zr, Ti), V (Nb, V, Ta), and VI (Cr, Mo, W). Because of the novel chemical compositions, HEAs have attracted considerable attention for use in high-temperature applications [13]-[29].

The importance of present research is that there is a great demand for enhancement of refractory materials operational temperature and development of the new class of metallic based refractory materials to replace the conventional such as Ni-base and Co-based as well as steel-based alloys. The thermo-mechanical processing is a well-known process that affects the development of microstructure, texture, and mechanical properties. Therefore, the application of thermo-mechanical processing on TaHfNbZrTi RHEA is expected to alter the deformation and annealing microstructures and also enhance furthermore of desired properties. There was no deformation and very high-temperature annealing up to 1400 °C studies available on TaHfNbZrTi equiatomic RHEA. The present investigation will contribute to understanding and remain a reference for future studies on heavy deformation and high-temperature heat-treated microstructure and texture evolution of RHEAs.

II. Experimental Procedure

A. Processing

Veeresham Mokali is with Indian Institute of Technology Hyderabad, India (e-mail: mokaliveeresham@gmail.com).

The equiatomic TaHfNbZrTi RHEA was prepared through an argon arc melting furnace, starting with Ta, Hf, Nb, Zr, and Ti high purity constituent elements. Re-melting was done several times for achieving homogeneous mixing of elements. The as-cast block of the TaHfNbZrTi alloy surface was polished mechanically and then cold-rolled up to 50% (CR – 50%). Afterward, the cold-rolled 50% sample was sealed in the quartz tube under vacuum, and the tube is filled with small Ti chips in order to prohibit oxidation of specimens in the heat treatment. Subsequently, 50% cold-rolled sample is heat-treated at 1400 °C temperature for 10 min. This processing was carried out to modify and refine the as-cast microstructure where the as-cast specimen consists of coarse and dendritic microstructure. Eventually, this specimen further cold-rolled up to 90% (CR – 90%) reduction in thickness several passes. The cold-rolled TaHfNbZrTi specimens were sealed in the quartz tube under vacuum and tube filled with small Ti chips in order to prohibit oxidation of specimens in the annealing treatment. The cold-rolled 90% RHEA specimens are subjected to various temperatures 800 °C, 1000 °C, 1250 °C, and 1400 °C for 1 h followed by quenching immediately in water. These cold-rolled and annealed specimens of TaHfNbZrTi RHEA were further characterized by using the SEM-EBSD technique.

B. Characterization

The cold-rolled 90% and annealed microstructural and textural studies of TaHfNbZrTi RHEA specimens were carried out by utilizing an electron backscatter diffraction (SEM-EBSD) attached to a scanning electron microscope (SEM: Carl-Zeiss, Germany; Model: SUPRA 40, EBSD: Oxford Instruments, UK). The RHEA specimens for EBSD experiments were prepared using mechanical polishing up to 2000 grade emery paper and then followed by electropolishing at 18.5-20 Volt and current 1.3-2.2 Amp in the methanol and perchloric acid with 9:1 ratio by the volume electrolyte solution. The AztecHKL software (Oxford Instruments, UK) was used to acquire EBSD scans. For analyzing further, the EBSD dataset, which was acquired earlier, was exported to the TSL-OIM™ software (EDAX Inc., USA). The ODFs (Orientation Distribution Functions) from the EBSD dataset were processed utilizing the harmonic series expansion method (series rank = 22). The ODFs volume fractions of important texture components were determined by a 15° degrees' cut-off angle.

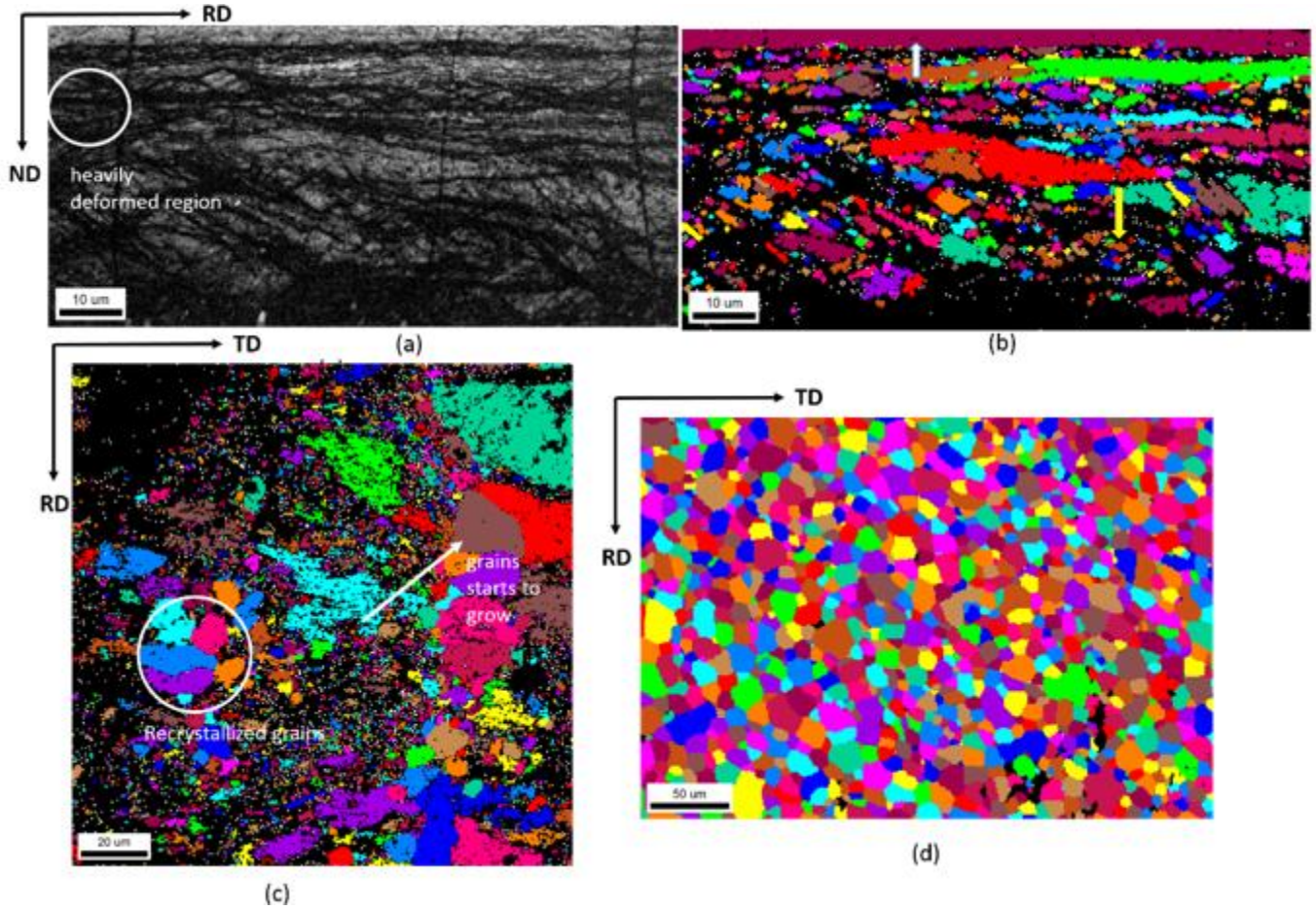

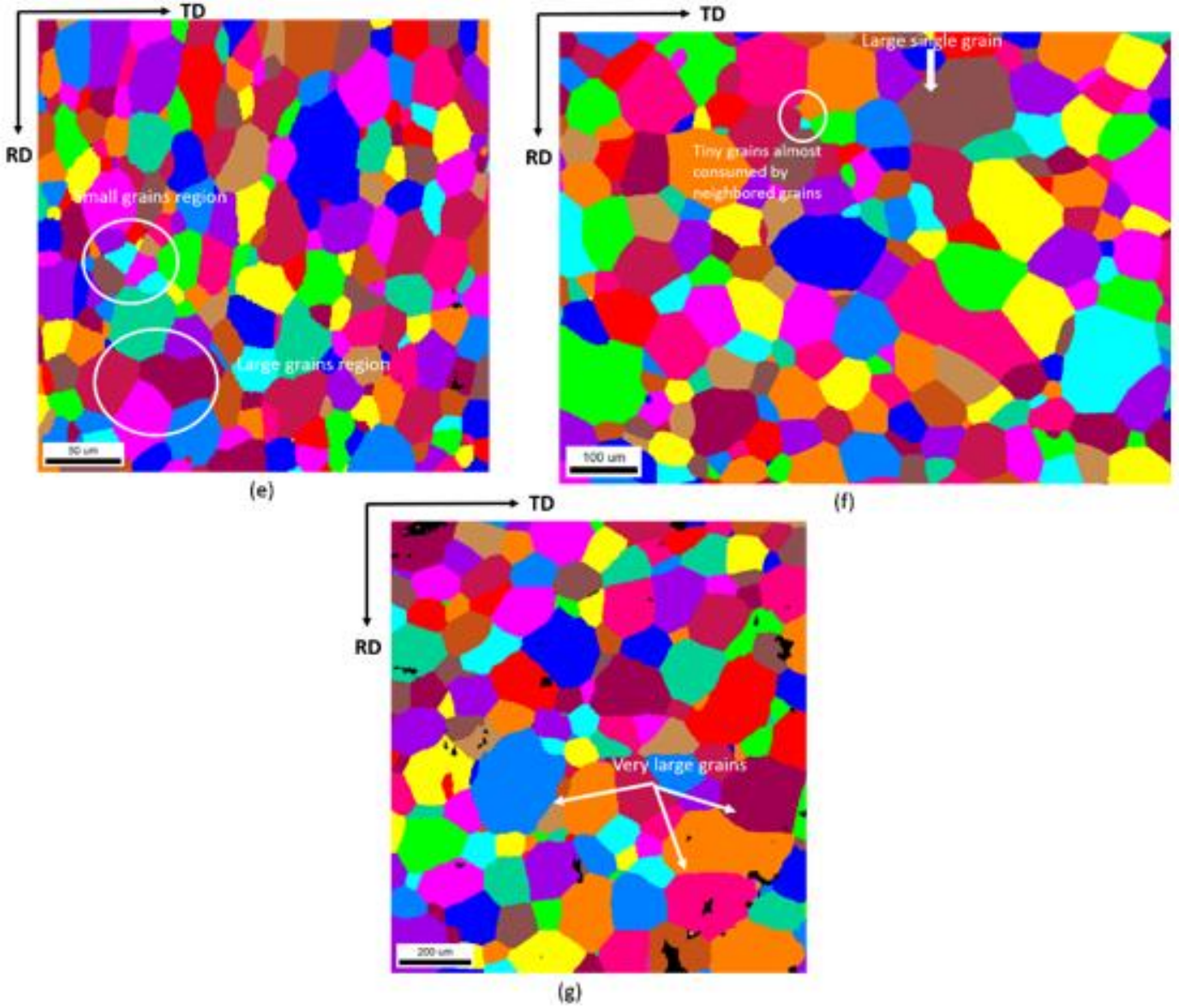

Fig. 1 (a), (b) IQ map and unique grain color map of cold-rolled 90% along RD-ND plane, (c)-(g), EBSD unique grain color maps annealed at various temperatures ranging from 800 ºC to 1400 ºC along TD-RD plane, (c) 800 ºC, (d) 850 ºC, (e) 1000 ºC, (f) 1250 ºC, (g) 1400 ºC for 1 h

III. Results

A. Evolution of Severely Cold-rolled Microstructure and Texture of TaHfNbZrTi

Figs. 1 (a) and (b) are image quality (IQ) map and unique grain color map of cold-rolled 90% along RD-ND plane of TaHfNbZrTi alloy obtained by SEM-EBSD. The heavily cold-rolled microstructure reveals a very fine microstructure development that has an average grain size of ~1.59 µm (Table I). Severely deformed (cold-rolled 90%) microstructure shows the development of deformation microstructural heterogeneity regions of fine grains, elongated flatten grains inclined towards the rolling direction (indicated with white arrow), and heavily deformed region (shown inside the white circle), and also the formation of heavily shear bands and deformation bands.

Fig. 2 (a) is the φ_2 = 45° section of the ODF of 90% cold-rolled sample. The crystallographic texture from the ODF section cold-rolled 90% clearly reveals RD fiber's presence and weak ND fiber texture. The maximum intensity is present at {100} <1-10>, which is an important texture component of RD fiber.

B. Evolution of Annealed Microstructure and Texture of TaHfNbZrTi

Figs. 1 (c)-(g) show representative microstructures of severely cold-rolled 90% specimens after isochronal annealing (for 1 h) at various temperatures in the range of 800 °C-400 °C. The evolution of rolled condition, and annealed temperatures microstructure and texture were determined by SEM-EBSD observations. The microstructure of annealed at 800 °C for 1 h (Fig. 1 (c)), which clearly exhibits partial recrystallization, reveals the presence of unrecrystallized and recrystallized regions in the microstructure. The recrystallized areas in the microstructure have very fine grain clusters shown in the circle.

Further, coarsening of recrystallized grains by following the grain growth process is indicated with arrows, the microstructure has an average grain size of ~1.56 µm (Table I). Furthermore, the CR-90% TaHfNbZrTi RHEA alloy annealed at temperature 850 °C for 1 h, slightly higher temperature than previously annealed temperature (Fig. 1 (d)), shows that the complete recrystallized microstructure has an average grain size of ~8.67 µm (Table I), grain growth witnessed nearly six times incensement than previously annealed temperature, and interestingly microstructure featured with almost nearly equal grain sizes and distributed homogenously. Therefore, further heavily deformed (CR-90%) specimen annealed at 1000 °C temperature for 1 h (Fig. 1 (e)) featured with complete recrystallized microstructure as previously annealed temperature. In addition to that, the development of coarse microstructure and distribution varying grain sizes was noticed. The microstructure has the inhomogeneous distribution of grain sizes, the presence of regions with small and large grains in the microstructure is shown with circles and arrows in the figure, respectively. This clearly reveals that larger grains were consuming smaller grains, such phenomena are commonly noticed during grain growth. Including these equiaxed grains developed in some microstructure regions, the average grain size is observed at around ~17.9 µm. Furthermore, (Fig. 1 (f)) is the microstructure of annealed condition at 1250 °C for 1 h after CR-90% of TaHfNbZrTi alloy. In this case, a similar trend has been followed in terms of microstructure development as like 1000 °C temperature with nearly three times enhancement in the average grain size up to ~48.6 µm (Table I). 1250 °C annealed microstructure clearly reveals almost completely the consumption of small grains by large surrounding grains (circled marking). Similarly, like conditions annealed at 1000 °C and 1250 °C, the abnormal grain growth continued to exhibit for annealed at 1400 °C for 1 h (Fig. 1 (g)), apart from this the grains were grown very larger due to the effect of extremely high annealing temperature; the average grain size is 84.04 µm (Table I). It is clear that the average grain size increases with annealing temperature. Thus, more interestingly, the formation of five and six-sided facet equiaxed grains were the most common microstructural features noticed in the range of 850 °C and 1400 °C annealed conditions.

The annealing texture in the range of 800 °C to 1400 °C temperatures acquired after cold rolling 90% TaHfNbZrTi RHEA is shown by $\phi2 = 45^{o}$ constant ODF section in Figs. 2 (b)-(f). The CR-90% of TaHfNbZrTi sample annealed at 800 °C temperature for 1 h (Fig. 2 (b)) saw the development of strong continuous normal to rolling direction (ND) and weak rolling direction (RD) fiber texture. The maximum ODF intensity shows a shift to the left from ND fiber texture components. Further 90% cold-rolled TaHfNbZrTi RHEA specimen annealed at 850 °C for 1 h (Fig. 2 (c)) shows the development of ND fiber texture and the improvement of RD fiber texture. Subsequently, cold-rolled 90% sample annealed at 1000 °C for 1 h (Fig. 2 (d)) shows the evolution of strong ND fiber texture weak RD fiber texture maximum intensities of ND fiber seen at {111} <110> component. And therefore, a severely cold-rolled specimen annealed at 1250 °C for 1 h (Fig. 2 (e)) shows very weak ND fiber texture development and also revealed the evolution of RD fiber and other non-important BCC texture components. After that, further TaHfNbZrTi RHEA heavily cold-rolled specimen annealed at high temperature 1400 °C for 1 h (Fig. 2 (f)) $\phi2 = 45^{o}$ constant ODF section reveals the evolution of discontinues ND fiber texture and contours with less intensities are distributed at various locations.

TABLE I
AVERAGE GRAIN SIZE OF COLD-ROLLED 90%, AND ANNEALING TREATED AT DIFFERENT TEMPERATURES RANGING FROM 800 °C TO 1400 °C FOR 1 H

	CR-90	800 °C	850 °C	1000 °C	1250 °C	1400 °C
Grainsize (µm)	01.59	01.56	08.67	17.90	48.60	84.04
Standard Deviation	01.46	01.90	04.45	10.19	29.83	55.05

IV. DISCUSSION

The ultrafine-grained (UFG) microstructure can be introduced into engineering materials via heavy rolling (severe plastic deformation). The development of microstructure in the metallic materials during heavy rolling, in terms of large strain deformation, is manifested by grain subdivision at different dimensions assisted by the evolution of very fine grain size, even nanoscale microstructure. The microstructural heterogeneity induced during the severe rolling process such as deformation bands, shear bands, and the local texture evolution proceeds due to the rotation of different parts of each grain in the microstructure to distinct end orientations within the grain because of inhomogeneous strain distribution. The enhancement of deformation strain can convert LAGBs into deformation-induced HAGBs to accommodate dislocations and immense strain. The grain subdivision results in an increment of finer grain size [30], eventually accommodating large deformation strain. The heavy deformation introduces high strain regions, and heterogeneity in microstructure can be described as a non-equilibrium configuration because of the high density of dislocations. The annealing is often needed to convert them into equiaxed strain-free grains. In the present work, partial recrystallization at 800 °C for 1 h is expected due to the annealed temperature being lower than the recrystallization temperature. However, the partial recrystallized microstructure feature consists of both recrystallized and non-recrystallized regions. The recrystallized regions contain grain sizes much coarser whereas in the non-recrystallized regions the retention of deformed structure would prevail. When the cold-rolled sample is subjected to annealing at 850 °C for 1 h, where the annealing temperature slightly increased than the previous annealing temperature, the microstructure evidences the complete recrystallization. The annealed temperature could be above the recrystallization temperature. The deformation structure was found to evolve into a uniform and nearly homogeneous equiaxed grain structure. However, some “abnormal” grains appear in the specimens annealed at temperatures ranging from 1000 °C to 1400 °C. The microstructural inhomogeneity of annealed in the

range of 1000 °C to 1400 °C temperatures interestingly shows fine grains and extremely large grains, which are almost equiaxed grains developed in the process of grain growth and abnormal grain growth mechanism which was discussed previously. The increase in annealing temperature assists the increase in average grain size and irregular grains, turning into five and six-sided facet grains. Such facet grains were seen at annealing temperatures ranging from 850 °C to 1400 °C. The facet formation might be due to the existence of curvature effect of grain boundaries and large stored energy, which assist simultaneously the development of facet boundaries and boundary motion results in coarsening of grains and formation of facet equiaxed grains [31], [32]. An enhancement in grain growth and facet grain formation in the annealing process has been attributed to unstable grain boundaries helping greater mobility of boundaries.

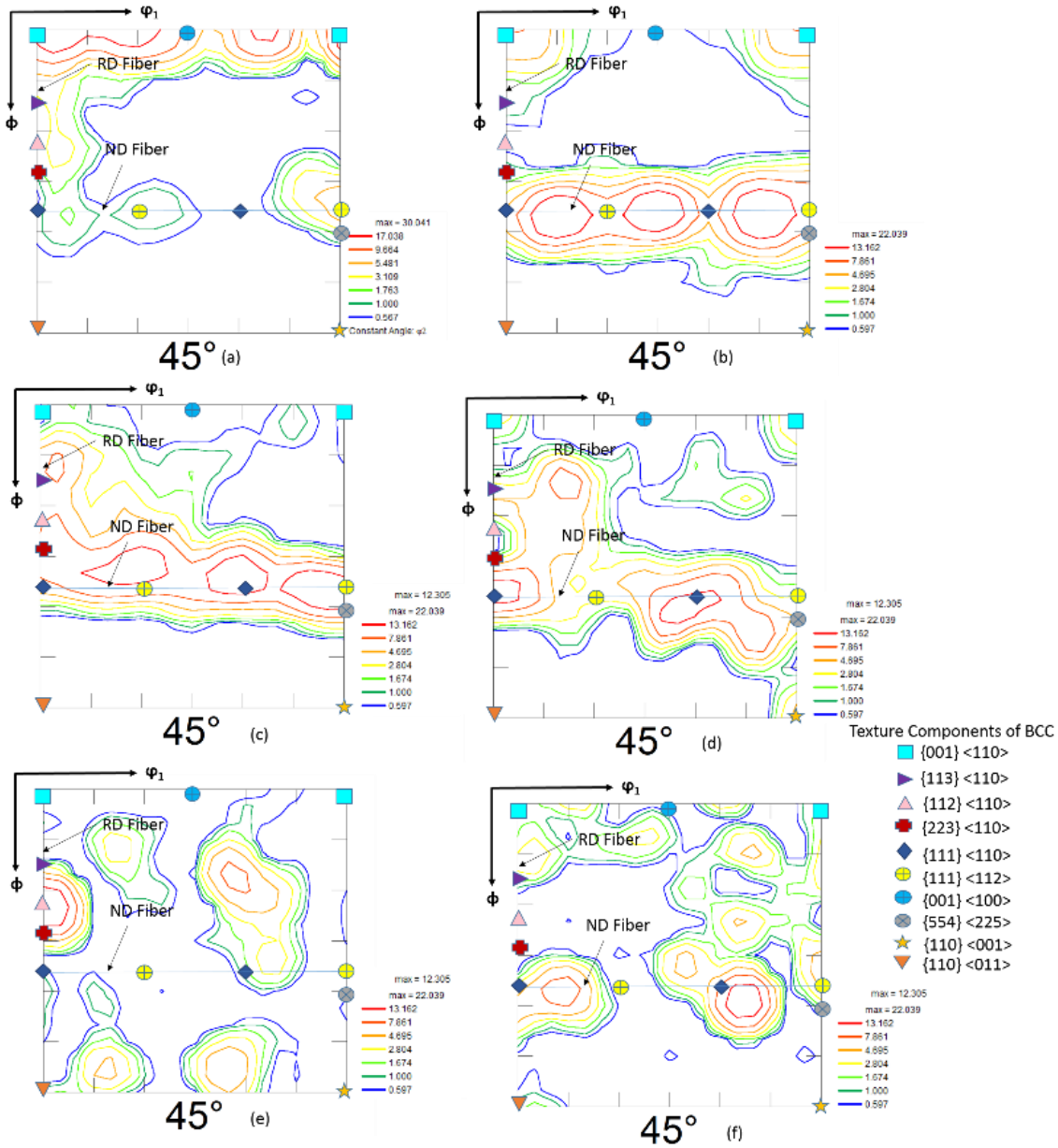

Fig. 2 (a) ϕ2 = 45º sections of ODFs of cold-rolled 90%, and (b)-(f) ϕ2 = 45º sections of ODFs of annealed in the range of 800 ºC to 1400 ºC temperatures, (b) 800 ºC, (c) 850 ºC, (d) 1000 ºC, (e) 1250 ºC, and (f) 1400 ºC for 1 h

The development of cold-rolling and annealing texture in BCC materials is extensively explored in several steels and other alloys. The single-phase BCC materials were characterized by the evolution of RD and ND fibers (RD//<110> and ND//<111>) [32]. The development of the RDs-fiber important components including (001) [1]-[10], (113) [1]-[10], (112) [1]-[10] and (223) [1]-[10] rises uniformly up to 70% rolling process. However, (112) [1]-[10], and (111) [1]-[10] important components of RD-fiber will tend to strengthen further increase in rolling reduction above 70%. In the case of the ND-fiber texture, it does not develop significantly up to 80% rolling. Moreover, with further rolling, the ND-fiber component would strengthen preferentially [32]. The ND-fiber texture components strengthening after annealing

treatment can be favored by the recrystallization process; it is commonly observed in BCC materials. The high stored energy of ND-fiber texture components is usually easily recrystallized, and the deformed RD-fiber components would exhibit recovery behavior [33]. This results in ND-fiber strengthening than the RD-fiber components after recrystallization. In the case of present investigated refractory TaHfNbZrTi HEA after CR 90% and annealing treatments at various temperatures from 800 °C to 1400 °C observed mostly the development of RD and ND fiber texture except for the annealing treatment at 1250 °C temperature. However, the details of the development of weak ND fiber texture might be clearly understood by the origin of preferential texture components and their growth process through TEM studies.

V. Conclusion

The equiatomic TaHfNbZrTi RHEA severely deformed up to cold-rolled - 90% reduction in thickness and subsequently annealed in the range of 800 °C-1400 °C temperatures. The evolution of severely cold-rolled TaHfNbZrTi RHEA microstructure was featured by deformation inhomogeneity such as extensive deformation banding, shear bands, and the microstructure was severely fragmentation by fine-scale helped in the formation of very fine grains. The development of ND and RD fiber texture is observed when the TaHfNbZrTi alloy was rolled to a 90% reduction in thickness. Therefore, heat-treated CR-90% RHEA at 800 °C temperature for 1 h showed partially recrystallized microstructure. However, a complete recrystallized microstructure is achieved at 850 °C annealed temperature. Simultaneously grain growth and abnormal grain growth started at 1000 °C, continued up to the annealed temperature 1400 °C. Recrystallization texture is prevailed for various annealed temperatures.

References

[1] Yeh, J. W., Chen, S. K., Lin, S. J., Gan, J. Y., Chin, T. S., Shun, T. T., ... & Chang, S. Y. (2004). Nanostructured high-entropy alloys with multiple principal elements: novel alloy design concepts and outcomes. Advanced Engineering Materials, 6(5), 299-303.

[2] Yeh, J.W., Alloy Design Strategies and Future Trends in High-Entropy Alloys. Jom, 2013.65(12): p. 1759-1771.

[3] Otto, F., Yang, Y., Bei, H., & George, E. P. (2013). Relative effects of enthalpy and entropy on the phase stability of equiatomic high-entropy alloys. Acta Materialia, 61(7), 2628- 2638.

[4] Yao, M. J., Pradeep, K. G., Tasan, C. C., & Raabe, D. (2014). A novel, single phase, non- equiatomic FeMnNiCoCr high-entropy alloy with exceptional phase stability and tensile ductility. Scripta Materialia, 72, 5-8.

[5] Zhang, Y., Zuo, T. T., Tang, Z., Gao, M. C., Dahmen, K. A., Liaw, P. K., & Lu, Z. P. (2014). Microstructures and properties of high-entropy alloys. Progress in Materials Science, 61, 1-93.

[6] Lu, Z. P., Wang, H., Chen, M. W., Baker, I., Yeh, J. W., Liu, C. T., & Nieh, T. G. (2015). An assessment on the future development of high-entropy alloys: summary from a recent workshop. Intermetallics, 66, 67-76.

[7] Tsai, M.-H. and J.-W. Yeh, High-Entropy Alloys: A Critical Review. Materials Research Letters, 2014. 2(3): p. 107-123.

[8] Gao, M.C., Progress in High-Entropy Alloys. Jom, 2014. 66(10): p. 1964-1965.

[9] Zhang, Z., Mao, M. M., Wang, J., Gludovatz, B., Zhang, Z., Mao, S. X., ... & Ritchie, R. O. (2015). Nanoscale origins of the damage tolerance of the high-entropy alloy CrMnFeCoNi. Nature communications, 6, 10143.

[10] Gludovatz, B., Hohenwarter, A., Catoor, D., Chang, E. H., George, E. P., & Ritchie, R. O. (2014). A fracture-resistant high-entropy alloy for cryogenic applications. Science, 345(6201), 1153-1158.

[11] Pickering, E.J. and N.G. Jones, High-entropy alloys: a critical assessment of their founding principles and future prospects. International Materials Reviews, 2016. 61(3): p. 183-202.

[12] Z., Pradeep, K. G., Deng, Y., Raabe, D., & Tasan, C. C. (2016). Metastable high- entropy dual-phase alloys overcome the strength–ductility trade-off. Nature, 534(7606), 227.

[13] Senkov, O. N., Wilks, G. B., Miracle, D. B., Chuang, C. P., & Liaw, P. K. (2010). Refractory high-entropy alloys. Intermetallics, 18(9), 1758-1765.

[14] Senkov, O.N., C. Woodward, and D.B. Miracle, Microstructure and Properties of Aluminum-Containing Refractory High-Entropy Alloys. Jom, 2014. 66(10): p. 2030-2042.

[15] Senkov, O.N., et al., Mechanical properties of low-density, refractory multi-principal element alloys of the Cr-Nb-Ti-V-Zr system. Materials Science and Engineering a- Structural Materials Properties Microstructure and Processing, 2013. 565: p. 51-62.

[16] Senkov, O. N., Senkova, S. V., Woodward, C., & Miracle, D. B. (2013). Low-density, refractory multi-principal element alloys of the Cr–Nb–Ti–V–Zr system: Microstructure and phase analysis. Acta Materialia, 61(5), 1545-1557.

[17] Gao, M. C., Carney, C. S., Doğan, Ö. N., Jablonksi, P. D., Hawk, J. A., & Alman, D. E. (2015). Design of refractory high-entropy alloys. Jom, 67(11), 2653-2669.

[18] Huang, H., Wu, Y., He, J., Wang, H., Liu, X., An, K., ... & Lu, Z. (2017). Phase-transformation ductilization of brittle high-entropy alloys via metastability engineering. Advanced Materials, 29(30), 1701678.

[19] Zou, Y., Maiti, S., Steurer, W., & Spolenak, R. (2014). Size-dependent plasticity in an Nb25Mo25Ta25W25 refractory high-entropy alloy. Acta Materialia, 65, 85-97.

[20] Sheikh, S., Shafeie, S., Hu, Q., Ahlström, J., Persson, C., Veselý, J., ... & Guo, S. (2016). Alloy design for intrinsically ductile refractory high-entropy alloys. Journal of Applied Physics, 120(16), 164902.

[21] Senkov, O. N., Scott, J. M., Senkova, S. V., Meisenkothen, F., Miracle, D. B., & Woodward, C. F. (2012). Microstructure and elevated temperature properties of a refractory TaNbHfZrTi alloy. Journal of Materials Science, 47(9), 4062-4074.

[22] Senkov, O. N., Wilks, G. B., Scott, J. M., & Miracle, D. B. (2011). Mechanical properties of Nb25Mo25Ta25W25 and V20Nb20Mo20Ta20W20 refractory high entropy alloys. Intermetallics, 19(5), 698-706.

[23] Senkov, O.N. and C.F. Woodward, Microstructure and properties of a refractory NbCrMo0.5Ta0.5TiZr alloy. Materials Science and Engineering a-Structural Materials Properties Microstructure and Processing, 2011. 529: p. 311-320.

[24] Dimiduk, D. M., Woodward, C., Miracle, D. B., Senkov, O. N., & Senkova, S. V. (2012), Oxidation behavior of a refractory NbCrMo0.5Ta0.5TiZr alloy. Journal of Materials Science, 2012. 47(18): p. 6522-6534.

[25] Gorr, B., Azim, M., Christ, H. J., Mueller, T., Schliephake, D., & Heilmaier, M. (2015). Phase equilibria, microstructure, and high temperature oxidation resistance of novel refractory high-entropy alloys. Journal of Alloys and Compounds, 624, 270-278.

[26] Juan, C. C., Tsai, M. H., Tsai, C. W., Lin, C. M., Wang, W. R., Yang, C. C., ... & Yeh, J. W. (2015). Enhanced mechanical properties of HfMoTaTiZr and HfMoNbTaTiZr refractory high-entropy alloys. Intermetallics, 62, 76-83.

[27] Wu, Y. D., Cai, Y. H., Wang, T., Si, J. J., Zhu, J., Wang, Y. D., & Hui, X. D. (2014). A refractory Hf25Nb25Ti25Zr25 high-entropy alloy with excellent structural stability and tensile properties. Materials Letters, 130, 277-280.

[28] Senkov, O. N., Scott, J. M., Senkova, S. V., Miracle, D. B., & Woodward, C. F. (2011). Microstructure and room temperature properties of a high-entropy TaNbHfZrTi alloy. Journal of alloys and compounds, 509(20), 6043-6048.

[29] Eleti, R. R., Raju, V., Veerasham, M., Reddy, S. R., & Bhattacharjee, P. P. (2018). Influence of strain on the formation of cold-rolling and grain growth textures of an equiatomic HfZrTiTaNb refractory high entropy alloy. Materials Characterization, 136, 286-292.

[30] Hansen, N. and D.J. Jensen, Development of microstructure in FCC metals during cold work. Philosophical Transactions of the Royal Society of London Series a-Mathematical Physical and Engineering Sciences, 1999. 357(1756): p. 1447-1469.

[31] Pa, M., DP, D., Chandra, T., & CR, K. (1996). Grain growth predictions in microalloyed steels. ISIJ international, 36(2), 194-200.

[32] Humphreys, F.J. and M. Hatherly, in Recrystallization and Related Annealing Phenomena (Second Edition). 2004, Elsevier: Oxford.
[33] Verlinden, B., Driver, J., Samajdar, I., & Doherty, R. D. (2007). Thermo-mechanical processing of metallic materials (Vol. 11). Elsevier.